Behavioral/Systems/Cognitive

Direct GABAergic and Glycinergic Inhibition of the Substantia Gelatinosa from the Rostral Ventromedial Medulla Revealed by *In Vivo* Patch-Clamp Analysis in Rats

Go Kato,[1,2] Toshiharu Yasaka,[1] Toshihiko Katafuchi,[1] Hidemasa Furue,[1] Masaharu Mizuno,[3] Yukihide Iwamoto,[2] and Megumu Yoshimura[1]

Departments of [1]Integrative Physiology and [2]Orthopedic Surgery, Graduate School of Medical Sciences, Kyushu University, Fukuoka 812-8582, Japan, and [3]Division of Higher Brain Functions, Department of Brain Science and Engineering, Graduate School of Life Science and Systems Engineering, Kyushu Institute of Technology, Kitakyushu 808-0196, Japan

Stimulation of the rostral ventromedial medulla (RVM) is believed to exert analgesic effects through the activation of the serotonergic system descending to the spinal dorsal horn; however, how nociceptive transmission is modulated by the descending system has not been fully clarified. To investigate the inhibitory mechanisms affected by the RVM, an *in vivo* patch-clamp technique was used to record IPSCs from the substantia gelatinosa (SG) of the spinal cord evoked by chemical (glutamate injection) and electrical stimulation (ES) of the RVM in adult rats. In the voltage-clamp mode, the RVM glutamate injection and RVM-ES produced an increase in both the frequency and amplitude of IPSCs in SG neurons that was not blocked by glutamate receptor antagonists. Serotonin receptor antagonists were unexpectedly without effect, but a $GABA_A$ receptor antagonist, bicuculline, or a glycine receptor antagonist, strychnine, completely suppressed the RVM stimulation-induced increase in IPSCs. The RVM-ES-evoked IPSCs showed fixed latency and no failure at 20 Hz stimuli with a conduction velocity of >3 m/s (3.1–20.7 m/s), suggesting descending monosynaptic GABAergic and/or glycinergic inputs from the RVM to the SG through myelinated fibers. In the current-clamp mode, action potentials elicited by noxious mechanical stimuli applied to the receptive field of the ipsilateral hindlimb were suppressed by the RVM-ES in more than half of the neurons tested (63%; 10 of 16). These findings suggest that the RVM-mediated antinociceptive effects on noxious inputs to the SG may be exerted preferentially by the direct GABAergic and glycinergic pathways to the SG.

Key words: **descending inhibitory system; *in vivo* patch clamp; substantia gelatinosa; pain; GABA; glycine**

Introduction

Several studies have demonstrated that stimulation of the rostral ventromedial medulla (RVM), including raphe nuclei such as the nucleus raphe magnus (NRM), the nucleus raphe pallidus (NRP), and the nucleus raphe obscurus, and adjacent nuclei of the reticular formation, such as the nucleus reticularis gigantocellularis (NGC) and the nucleus reticularis gigantocellularis pars α (NGCα), causes an apparent analgesic effect through the descending inhibitory pathway to the spinal cord in rats (Oleson et al., 1978; Azami et al., 1982; Brodie and Proudfit, 1984; Light et al., 1986). Classically, the descending RVM system was considered to consist mainly of a serotonergic system (Bowker et al., 1981); however, recent studies have revealed that the raphe nuclei are not homogeneous populations of serotonergic neurons. For example, the spinal projections of the GABAergic and/or glycinergic neurons from the RVM are also suggested to contribute to the modulation of spinal sensory systems (Sorkin et al., 1993; Antal et al., 1996; Millan, 2002). In addition, the coexistence of other neurotransmitters such as GABA, somatostatin, and enkephalin has been demonstrated in raphe-spinal serotonergic neurons (Millhorn et al., 1987, 1988; Bowker and Abbott, 1988; Reddy et al., 1990; Jones et al., 1991; Millan, 2002). Although these neuroanatomical studies have shown direct projections of descending pathways containing multiple neurotransmitters, the functional significance of these pathways in the spinal dorsal horn has not been demonstrated.

The superficial dorsal horn, especially the substantia gelatinosa [(SG) lamina II] of the spinal cord (Rexed, 1952), is implicated in nociceptive processing, because small myelinated Aδ-afferent and unmyelinated C-afferent fibers that convey predominantly noxious sensation make synaptic contacts with SG neurons (Kumazawa and Perl, 1978; Cervero and Iggo, 1980; Sugiura et al., 1986; Yoshimura and Jessell, 1989; Yoshimura, 1996). To characterize the descending inhibitory pathway from the RVM in this study, we recorded IPSCs of SG neurons by means of the *in vivo* patch-clamp technique and examined the

Received Nov. 10, 2005; revised Dec. 23, 2005; accepted Dec. 26, 2005.

This work was supported by grants-in-aid for scientific research (15029247, 15300135, and 17590207) to M. Y., H. F., and T. K., respectively, from the Japanese Ministry of Education, Culture, Sports, Science and Technology, and by the 21st Century Center of Excellence Program to M. Y. We thank Dr. A. M. Strassman for reading this manuscript and H. Mizuguchi for histological support.

Correspondence should be addressed to Toshihiko Katafuchi, Department of Integrative Physiology, Graduate School of Medical Sciences, Kyushu University, Fukuoka 812-8582, Japan. E-mail: kataf@physiol.med.kyushu-u.ac.jp.

DOI:10.1523/JNEUROSCI.4856-05.2006

 0270-6474/06/261787-08$15.00/0

effects of chemical and electrical stimulation (ES) of the RVM. Furthermore, the pharmacological characteristics of the RVM stimulation-evoked IPSCs (eIPSCs) and their physiological significance in the noxious stimuli-induced responses of SG neurons were also investigated.

Materials and Methods

All experimental procedures involving the use of animals were approved by the Ethics Committee on Animal Experiments, Kyushu University.

Insertion of microinjection cannula and stimulus electrode. Male Sprague Dawley rats (8–11 weeks of age; 280–360 g) were anesthetized with urethane (1.2–1.5 g/kg, i.p.). A burr hole was made in the skull, and the 25 gauge [0.5 mm outer diameter (OD)] guide cannula was inserted 2 mm above the RVM and fixed to the skull by dental cement. The stimulating sites were aimed mainly at the raphe nuclei (NRM and NRP; stereotaxic coordinates: 10.3–11.3 mm posterior to bregma; midline, 7.5–8.0 mm ventral to dura) (Paxinos and Watson, 2005). An injection cannula (33 gauge; 0.21 mm OD) or concentric bipolar stimulating electrode (0.2 mm OD; model IMB-9002; Inter Medical Company, Nagoya, Japan) was inserted through this guide cannula. The injection cannula and stimulation electrode were equipped with stoppers to extend 2 mm beyond the tip of the guide cannula (see Fig. 1*A*).

Preparation for the in vivo *patch-clamp recording.* The methods used for the *in vivo* patch-clamp recording were similar to those described previously (Furue et al., 1999; Narikawa et al., 2000; Sonohata et al., 2004). Under urethane anesthesia, oxygen was supplied through a nose cone. Artificial ventilation of the pneumothorax was not performed, as reported previously (Sonohata et al., 2004). If a withdrawal reflex to the noxious stimuli appeared, an additional dose of urethane was given during surgery and the data collection period. The rectal temperature was kept at 37−38°C by a heating pad. A thoracolumbar laminectomy was performed exposing the level from L1 to L6, and then the rat was placed in a stereotaxic apparatus (model ST-7; Narishige, Tokyo, Japan). After the dura was removed, a dorsal root that enters the spinal cord above the level of the recording sites was retracted with a small glass hook, and the pia-arachnoid membrane was cut to make an opening large enough to allow a patch electrode to enter the SG from the surface of the spinal cord. The surface of the spinal cord was irrigated with 95% O_2–5% CO_2-equilibrated Krebs' solution (15 ml/min) containing the following (in mM): 117 NaCl, 3.6 KCl, 2.5 $CaCl_2$, 1.2 $MgCl_2$, 1.2 NaH_2PO_4, 11 glucose, and 25 $NaHCO_3$, through glass pipettes at 38 ± 1°C. An experimental set up for the *in vivo* patch-clamp recording is illustrated in Figure 1*A*.

Patch-clamp recordings. Whole-cell voltage-clamp recordings were obtained from SG neurons with a patch electrode that had tip resistance of 8–12 MΩ and was filled with a pipette solution having the following composition (in mM): 110 Cs_2SO_4, 5 TEA-Cl, 0.5 $CaCl_2$, 2 $MgCl_2$, 5 EGTA, 5 HEPES, and 5 Mg-ATP, in the voltage-clamp mode to observe GABAergic and/or glycinergic IPSCs, or with 136 K-gluconate, 5 KCl, 0.5 $CaCl_2$, 2 $MgCl_2$, 5 EGTA, 5 HEPES, and 5 Mg-ATP, mainly in the current-clamp mode. In some cases, however, the pipette solution containing K-gluconate was also used in the voltage-clamp mode to observe EPSCs and slow membrane currents. Signals were acquired with a patch-clamp amplifier (Axopatch 200B; Molecular Devices, Union City, CA). The data were digitized with an analog-to-digital converter (Digidata 1321A, Molecular Devices), stored on a personal computer with a data acquisition program (Clampex version 8.0; Molecular Devices), and analyzed with a special software package (Clampfit version 4.1; Molecular Devices). In voltage-clamp mode, the holding potential was 0 mV, at which glutamate-mediated EPSCs were negligible (Yoshimura and Nishi, 1993). Frequencies and amplitudes of spontaneous IPSCs (sIPSCs) and miniature IPSCs were measured automatically with MiniAnalysis software (Synaptosoft, Decatur, GA). The amplitude of each postsynaptic current was measured from the initial inflection point (not from the baseline) to the peak to avoid the effects of temporal summation on the amplitude distribution. Artifacts produced by RVM-ES were completely excluded from IPCS amplitude and frequency analysis by their short duration. The validity of this method was confirmed by visual inspection of all traces on a fast time scale before they were accepted for further analysis.

Glutamate injection into the RVM. Monosodium-L-glutamate (30 nmol; Nacalai Tesque, Kyoto, Japan) was injected manually (0.3 μl/min) with a microsyringe (no. 80100; Hamilton, Reno, NV) into the RVM in a volume of 0.3 μl via an injection cannula. The injection of the drug was monitored continuously by following the movement of an air bubble in a tube between the injection syringe and the injection cannula.

Electrical stimulation of the RVM. The electrical stimulation was performed with rectangular pulses (duration, 100 μs; intensity, 10–100 μA; frequency, 0.1–100 Hz). It has been shown that the largest current spread may be up to 1 mm away from the electrode with this intensity (Hentall and Fields, 1979; Light et al., 1986). The greater intensity of stimulation was not performed to avoid the large pulsation of the spinal cord caused by breathing.

Application of drugs. Drugs dissolved in Krebs' solution were applied to the surface of the spinal cord through inlet and outlet glass pipettes (see Fig. 1*A*) by exchanging solutions via a three-way stopcock without any change in either the perfusion rate or the temperature. The time necessary for the solution to flow from the stopcock to the surface of the spinal cord was ~5 s. The drugs applied were 6-cyano-7-nitroquinoxaline-2,3-dione (CNQX) (Tocris Cookson, St. Louis, MO), DL-2-amino-5-phosphonovaleric acid (APV) (Sigma, St. Louis, MO), strychnine (Sigma), bicuculline (Sigma), methysergide maleate salt (Sigma), ketanserin (Sigma), ondansetron (LKT Laboratories, St. Paul, MN), and RS 23597–190 hydrochloride (Tocris Cookson). The effectiveness of the drugs applied in the same way under *in vivo* conditions was confirmed in our previous study (Sonohata et al., 2004).

Pinch stimulation. The noxious mechanical stimuli were applied to the receptive field of the ipsilateral hindlimb with toothed forceps that were fixed on a rod, and various weights were put on the forceps. The frequency of EPSPs increased as the weight increased, and no significant accommodation was observed, thus indicating that the responses were mediated by the activation of nociceptors (Furue et al., 1999).

Identification of glutamate injection and electrical stimulation sites. After termination of electrophysiological recordings, rats were deeply anesthetized with supplemental urethane. Anodal electrolytic lesions were made by DC current (500 μA) through the electrode to mark the injection and stimulation sites. Transcardial perfusions with 4% paraformaldehyde in 0.1 M phosphate buffer (PB), pH 7.4, were performed. Brains were removed and immersed overnight in the same fixative solution at 4°C and rinsed in 0.1 M PB. Brains were cut into 50 μm sections with a cryostat and stained with cresyl violet.

Identification of SG neurons. Neurons were recorded at a depth of 30–150 μm from the dorsal surface of the spinal cord at the L2–S1 level of the spinal cord, which was within the SG when measured in the transverse slice (Furue et al., 1999). The recorded neurons were further identified in some instances by diffusion of neurobiotin into the cell through a patch pipette (0.1–0.2% in the electrode solution; Vector Laboratories, Burlingame, CA). After the electrophysiological recordings were terminated, the rats were deeply anesthetized with supplemental urethane and perfused transcardially with 4% paraformaldehyde in 0.1 M PB, pH 7.4. The spinal cord was removed and immersed overnight in the same fixative at 4°C, rinsed in 0.1 M PB, and sectioned parasagittally into 150 μm sections with a freezing vibratome. Free-floating sections were incubated overnight at 4°C in PBS with 0.3% Triton X-100 containing streptavidin–Texas Red (diluted 1:500; Jackson ImmunoResearch, West Grove, PA) and washed several times in PB. Some sections were further incubated with isolectin B4 (IB4) from *Bandeiraea simplicifolia* conjugated directly to fluorescein isothiocyanate (0.5 mg/ml; Sigma) to visualize the border between laminas II and III. The sections were mounted on gelatinized slides and viewed and photographed with an LSM 510 laser scanning confocal microscope (Zeiss, Oberkochen, German) (see Fig. 1*B*).

Statistical analysis. All numerical data were expressed as the mean ± SEM. Statistical significance was determined as $p < 0.05$ (and indicated by asterisks in the figures) by the *t* test (unless noted otherwise) for the absolute values of amplitude and frequency of IPSCs or by the Kolmogorov–Smirnov test for their probabilities. In all cases, *n* refers to the number of neurons tested. The membrane potentials were not corrected for the liquid junction potential between the Krebs' and patch-pipette solutions.

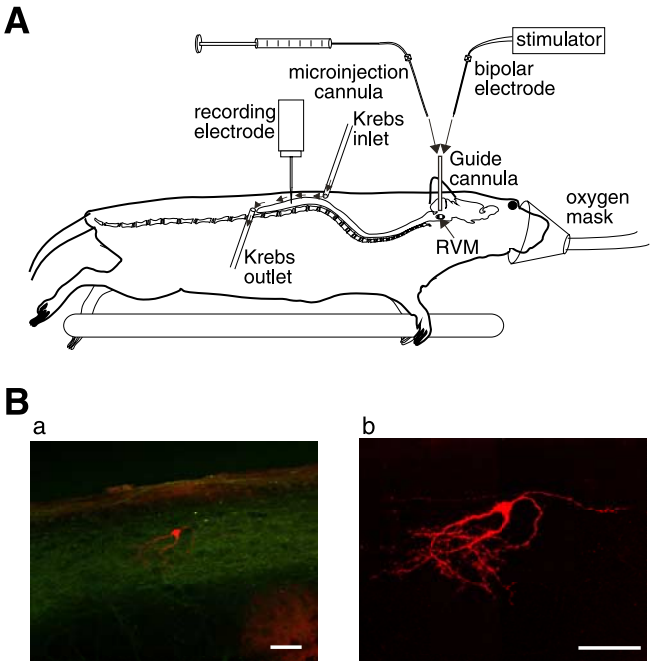

Figure 1. Schematic diagram of the *in vivo* rat preparation and histochemical identification of SG neurons. ***A***, While oxygen was supplied to a urethane-anesthetized rat from a nose cone, the lumbar spinal cord at the level from L1 to L6 was exposed by laminectomy. The surface of the spinal cord was perfused with 95% O_2–5% CO_2-equilibrated Krebs' solution (15 ml/min) from inlet to outlet glass pipettes at 38 ± 1°C (small arrows). ***Ba***, Representative SG neurons filled with neurobiotin from a patch pipette (red) that responded to the RVM-ES in a sagittal section of the spinal cord. Green fluorescence band shows IB4 binding, which indicates the inner layer of lamina II (SG). ***Bb***, The same neuron at a higher magnification. Scale bars, 50 μm.

Results

Stable recording was obtained from a single SG neuron for up to 4 h in a total of 166 SG neurons. All of the SG neurons examined had membrane potentials more negative than −53 mV. The average membrane potential and the input membrane resistance were −61.9 ± 0.5 mV (n = 166) and 376 ± 19 MΩ (n = 166), respectively. Under voltage-clamp conditions at a holding potential of −0 mV, SG neurons exhibited IPSCs with an average amplitude of 49 ± 4.1 pA (n = 77) and a frequency of 34.7 ± 1.6 Hz (n = 77). Application of the glutamate receptor antagonists CNQX and AP-5 had no significant effects on the amplitude and frequency of synaptic currents.

The neurons injected with neurobiotin (n = 20) were located in the dorsal part of the IB4 labeling (Fig. 1*Ba*), which has been demonstrated to be a marker of the inner lamina II (Silverman and Kruger, 1990). Neurons located deeper than the IB4 labeling were judged to be lamina III neurons and were excluded from the analysis. The SG neuron shown in Figure 1*Bb* possessed the morphological features of rounded soma with dendrites branching off ventrally, similar to the cells described previously as SG neurons with either Golgi staining (Beal and Bicknell, 1985) or horseradish peroxidase labeling (Woolf and Fitzgerald, 1983). Other types of SG neurons, such as those extending their dendrites rostrocaudally and radially, were also observed.

Facilitation of IPSCs by glutamate injection into the RVM

Glutamate injection into the RVM (RVM-GI) (100 mM; 0.3 μl; total, 30 nmol) increased both the frequency and amplitude of sIPSCs without inducing any outward current at the holding potential of 0 mV in 56% (5 of 9) of SG neurons tested (Fig. 2*A*). In the remaining neurons, RVM-GI did not alter the frequency or amplitude of sIPSCs (33%; 3 of 9) or reduce them (11%; 1 of 9). Figure 2*Ba–Bc* shows the corresponding traces in Figure 2*A* on an expanded time scale. The mean duration of the increase was 15.2 min (range, 1–35 min). Figure 2*C* shows cumulative probability plots for the interevent interval (left) and current amplitude (right) of sIPSCs. The RVM-GI shifted the distribution to higher frequencies and larger amplitudes of sIPSCs. The mean sIPSC frequency and amplitude were 134 ± 21% (n = 9) and 126 ± 10% (n = 9) of the control ($p < 0.05$), respectively (Fig. 2*C*, insets). The tip of the injection cannula was within the RVM in all cases. These results suggested that the activation of RVM neurons, but not the passing of fibers through the RVM, mainly facilitated sIPSCs in the SG.

Facilitation of IPSCs by RVM-ES

The RVM-ES (100 μs; 100 μA; 30 Hz) increased sIPSC frequency and amplitude in 71% (12 of 17) of the SG neurons tested, without any changes in baseline currents (Fig. 3*A*). Because neither slow outward nor inward current was observed even when the K-gluconate-containing pipette solution was used, we focused on IPSCs. At intensities <100 μA, the number of neurons that showed increased IPSCs was small, but the frequency itself was not changed. Although RVM-ES at low intensities (5–25 mA) has been reported to facilitate nociceptive transmission in the rat (Zhuo and Gebhart, 1997), there were no changes in EPSCs recorded with a K-gluconate-containing pipette solution during the RVM-ES at any stimulus intensities. The facilitation of IPSCs lasted only during the period of stimulation in most of the neurons, except for two cases in which the facilitation continued for 3 and 15 min after the RVM-ES. In the remaining neurons, the RVM-ES did not alter the frequency or amplitude of sIPSCs (29%; 5 of 17). Figure 3*Ba–Bc* shows the corresponding traces in Figure 3*A* on an expanded time scale. Figure 3*C* shows cumulative probability plots for the interevent interval (left) and current amplitude (right) of sIPSCs. The RVM-ES shifted the distribution to higher frequencies and larger amplitudes of sIPSCs. Under ES, the mean sIPSC frequency and mean amplitude were 122 ± 6% (n = 17) and 121 ± 7% (n = 17) of the control values ($p < 0.05$), respectively (Fig. 3*C*, insets), suggesting that the RVM-ES and the RVM-GI facilitate sIPSCs in the SG.

Involvement of $GABA_A$ and glycine receptors in the RVM-ES-eIPSCs

To investigate neurotransmitters responsible for the RVM-ES-induced changes in sIPSCs, the antagonist for glutamate, $GABA_A$, or glycine receptors were applied during RVM stimulation at 0.1 Hz. As shown in Figure 4*A*, the relative amplitude of the RVM-ES-induced IPSCs was not affected by simultaneous application of the AMPA and NMDA receptor antagonists CNQX (10 μM) and APV (25 μM) but was completely suppressed by the $GABA_A$ receptor antagonist bicuculline (20 μM) in a reversible manner. Figure 4*Ba–Bd* shows superimposed traces of the IPSCs at Figure 4*Aa–Ad*, respectively. The duration of the IPSCs blocked by bicuculline was relatively long (>24 ms; n = 12). On the other hand, as shown in Figure 4*C*, the RVM-ES-eIPSCs with a short duration (<13 ms; n = 6) (Fig. 4*D*) were not abolished by glutamate antagonists and bicuculline but were blocked by a glycinergic receptor antagonist, strychnine (2 μM). More than half of the monosynaptic eIPSCs were completely suppressed by either bicuculline or strychnine as shown in Figure 4. The remaining IPSCs, however, showed 80–90% suppression by either bicuculline or strychnine at the doses used, suggesting that some of them

were GABA or glycine dominant but involved both neurotransmitters. Because the glutamate antagonists (CNQX and APV) affected neither the amplitude nor frequency of IPSCs during the RVM-ES, we concluded that the RVM-ES-eIPSCs were mediated by monosynaptic $GABA_A$ and/or glycinergic receptors. Our previous studies have confirmed that drugs perfused on the surface of the spinal cord act equally on SG neurons, which are located within a range of 30 to 150 μm, as do those administered by bath application in slice preparations but not through systemic circulation (Furue et al., 1999; Sonohata et al., 2004).

No effect of 5-HT receptor antagonists on the RVM-ES-induced facilitation of IPSCs

Because GABA release in the spinal dorsal horn was enhanced by 5-HT through 5-HT_3 receptors (Alhaider et al., 1991; Peng et al., 2001; Hains et al., 2003; Kawamata et al., 2003), the effects of the 5-HT_3 receptor antagonist ondansetron on the RVM-ES (30 Hz)-induced facilitation of sIPSCs were examined. As shown in Figure 5, application of ondansetron did not affect either the control or the RVM-ES-induced facilitation of IPSCs. Figure 5*A* demonstrates the row traces of the RVM-ES-induced facilitation of sIPSCs without (left) and with (right) the application of ondansetron. In most cases, the single RVM-ES was followed by an IPSC (Fig. 5*A*, dots in middle two traces). As shown in Figure 5*B*, the RVM-ES-induced facilitation of the frequency and amplitude of sIPSCs was not affected by ondansetron. Figure 5*C* shows the mean sIPSC frequency (*a*) and mean amplitude (*b*) without or with the application of ondansetron. The frequency and amplitude of IPSCs during ondansetron were 147 ± 17% ($n = 7$) and 139 ± 13% ($n = 7$) of the control, respectively, whereas those without ondansetron were 147 ± 14% ($n = 7$) and 145 ± 10% ($n = 7$) ($p > 0.05$). Furthermore, other 5-HT receptor antagonists such as ketanserine (5-HT_{2A}-selective antagonist; $n = 4$), RS 23597–190 (5-HT_4 selective antagonist; $n = 3$), and methysergide (nonselective 5-HT antagonist; $n = 5$) were also without effect on the RVM-ES-mediated facilitation of sIPSCs (data not shown). These results suggested that the facilitation of sIPSCs during the RVM-ES was not mediated by 5-HT receptors.

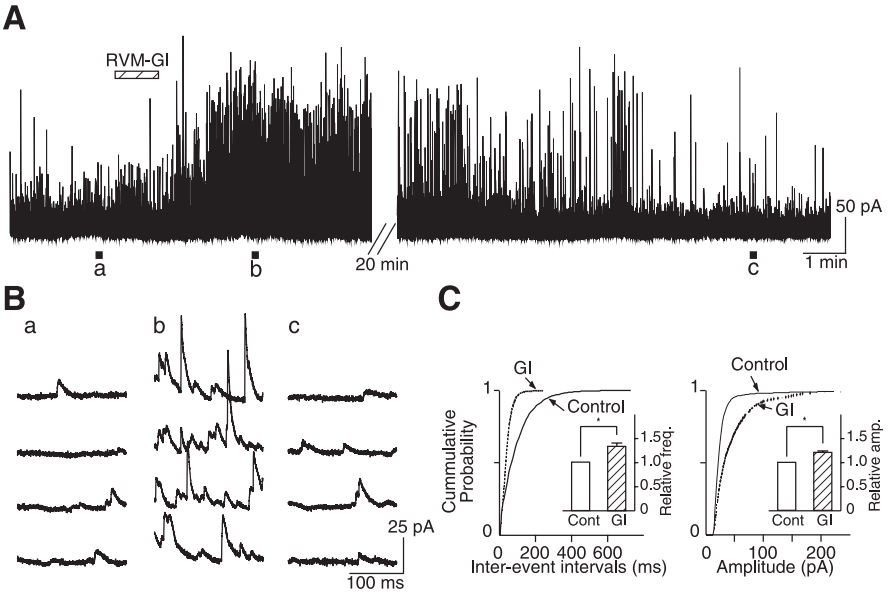

Figure 2. RVM-GI facilitates sIPSCs in the SG. ***A***, Typical example of the facilitation of sIPSCs induced by RVM-GI (30 nmol). ***Ba–Bc***, Corresponding traces on an expanded time scale in ***Aa–Ac***, respectively. ***C***, Cumulative distributions of interevent intervals (left; $p < 0.01$) and current amplitudes (right; $p < 0.05$) for sIPSCs recorded from the same neuron shown in ***A*** (2281 and 5801 events in a 200 s period for sIPSCs before and after RVM-GI). Insets, Averages of sIPSC amplitude (amp.) and frequency (freq.), which are normalized to their controls ($n = 9$). $^*p < 0.05$.

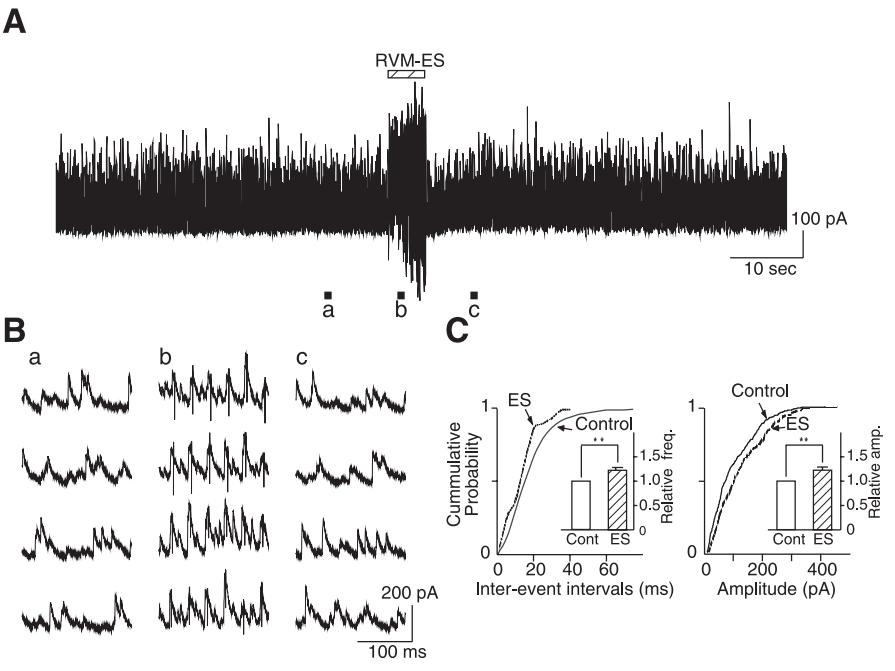

Figure 3. RVM-ES facilitates sIPSCs in the SG. ***A***, Typical example of the facilitation of sIPSCs induced by RMV-ES (100 μA; 30 Hz). ***B***, Three sets of traces (***a–c***) demonstrate IPSCs on an expanded time scale recorded before, during, and after RVM-ES, corresponding to ***a–c*** in ***A***. ***C***, Cumulative distributions of interevent intervals (left; $p < 0.05$) and current amplitudes (right; $p < 0.01$) for sIPSCs recorded from the same neuron shown in ***A*** (292 and 359 events in a 5 s period for sIPSCs before and after RVM-ES). Insets, Amplitudes (amp.) and frequencies (freq.) of sIPSCs are normalized to their controls ($n = 16$). $^{**}p < 0.01$.

Stimulus-frequency-dependent facilitation of sIPSCs by RVM-ES

Because every RVM-ES evoked an IPSC (Fig. 5*A*, dots), it was strongly suggested that the increase in frequency of IPSCs by the RVM-ES was caused by an increase in postsynaptic eIPSCs, depending on the stimulus frequency. As shown in Figure 6*A*, the RVM-ES-eIPSCs was always observed when the frequency was increased from 20 to 100 Hz. A stimulus-frequency-dependent increase in IPSC frequencies (Fig. 6*B*) was observed in all cases tested ($n = 4$). Furthermore, the RVM-eIPSCs showed a constant latency and no failure at 0.2 Hz (Fig. 6*C*, top) and 20 Hz (bottom; on a faster time scale), indicating that the RVM-ES-eIPSCs were monosynaptic in nature.

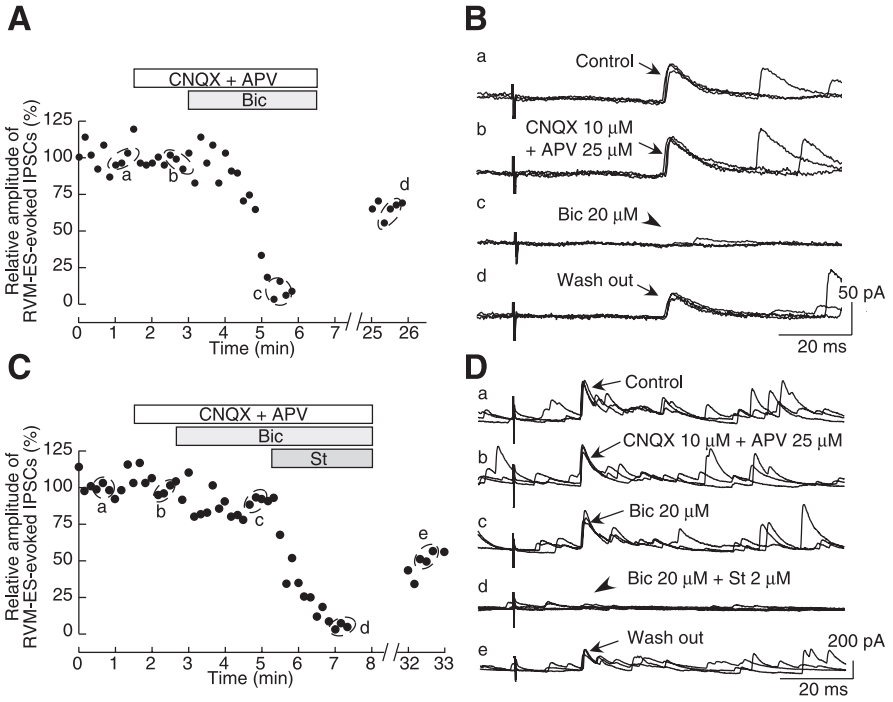

Figure 4. IPSCs evoked by RVM-ES are mediated by GABA or glycine. ***A***, Time course of the relative peak amplitude of the RVM-ES-eIPSCs. Simultaneous application of the AMPA and NMDA receptor antagonists CNQX (10 μM) and APV (25 μM) was without effect, but the $GABA_A$ receptor antagonist bicuculline (Bic; 20 μM) completely suppressed IPSCs in a reversible manner. ***Ba–Bd***, Superimposed traces of the IPSCs at ***a–d*** in ***A***. Note that the duration of the IPSCs was relatively long (>24 ms). ***C***, RVM-ES-eIPSCs that were not abolished by glutamate antagonists and bicuculline but were blocked by a glycinergic receptor antagonist, strychnine (St; 2 μM). ***Da–Dd***, Superimposed traces of the IPSCs with a short duration (<13 ms) at ***a–d*** in ***B***. The intensity and frequency of the RVM-ES were 100 μA and 0.1 Hz, respectively. Holding potential: 0 mV.

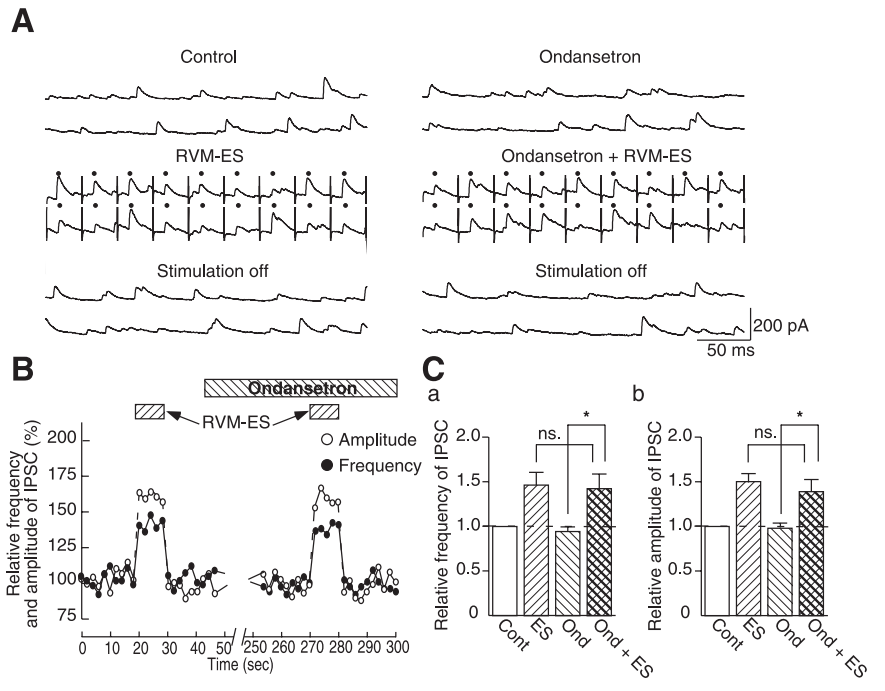

Figure 5. RVM-ES-mediated facilitation of sIPSCs was not blocked by a $5\text{-}HT_3$ receptor blocker. ***A***, Frequency and amplitude of sIPSCs were increased during RVM-ES in a reversible manner before drug application (left). The RVM-ES is always accompanied by IPSCs (dots). During application of a $5\text{-}HT_3$ receptor blocker, ondansetron, the facilitations were again observed (right). The stimulus intensity and frequency were 100 μA and 30 Hz, respectively. ***B***, Time courses of the frequency (filled circle) and amplitude (open circle). The enhancement of IPSCs induced by the RVM-ES was not affected by the application of ondansetron (20 μM). ***C***, Average amplitude and frequency of sIPSCs that are normalized to their controls ($n = 7$). ns., Not significant; Ond, ondansetron. *$p < 0.05$.

Location of the RVM-ES

Figure 7*A* demonstrates an example of a histological section showing an electrode placement within the RVM at 10.8 mm caudal to bregma. All of the electrical stimulation sites were within the RVM (Fig. 7*B*), in which 21 of 23 (88%) were in the raphe nuclei, such as NRM ($n = 15$) and NRP ($n = 6$), and 2 were in the NGCα. The monosynaptic IPSCs were elicited by the RVM-ES in 73% (11 of 15), 83% (5 of 6), and 100% (2 of 2) when the stimulation site was in the NRM, NRP, and NGCα, respectively. There was no clear topographic distribution of the GABAergic and glycinergic monosynaptic IPSCs in the RVM. As shown in Figure 7*C*, there were no differences in the conduction velocities (estimated from the latency and the distance between the RVM and the recording site) and peak amplitudes of GABAergic and glycinergic eIPSCs [6.4 ± 0.9 m/s and 133 ± 34.9 pA ($n = 12$) and 6.1 ± 1.3 m/s and 144 ± 41.9 pA ($n = 6$), respectively]. The conduction velocities were within the range of those of thin myelinated fibers.

Excitatory input elicited by cutaneous mechanical stimulation was abolished by RVM-ES

To investigate the functional significance of the RVM-ES in the spinal nociceptive transmission, five sets of pinch stimuli were applied for 5 s every 2 min to the receptive field of the ipsilateral hindlimb, and the RVM-ES was applied from 30 s before the third pinch stimuli for 1 min in the current-clamp mode (Fig. 8*A*). Figure 8*Ba–Bd* shows the corresponding traces in Figure 8*A* on an expanded time scale. As shown in Figure 8, *A* and *Ba*, pinch stimuli elicited a slight depolarization with a barrage of action potentials that disappeared within 1 s after the stimulation. The RVM-ES (100 μA; 30 Hz) elicited rapid hyperpolarization of the membrane potential (3–15 mV). The RVM-ES-induced hyperpolarization is considered to be caused by a summation of monosynaptic IPSPs, because the hyperpolarization occurred quickly after the start of the RVM-ES and continued during the RVM-ES. Pinch stimuli no longer induced action potentials when applied during the RVM-ES (Fig. 8*Bc*) and were observed again after the RVM-ES (Fig. 8*Bd*). The RVM-ES-evoked hyperpolarization and suppression of action potentials were observed in 63% (10 of 16) of the neurons tested.

Discussion

Previous studies have demonstrated that electrical and chemical stimulation of the

RVM or NRM result in an inhibition of spinal nociception (Fields et al., 1977; Belcher et al., 1978; Duggan and Griersmith, 1979; Rivot et al., 1980; Carstens et al., 1981; Hodge et al., 1983; Light et al., 1986; Zhuo and Gebhart, 1997). The mechanism of the antinociceptive effect is controversial, however, because many neurotransmitters in addition to 5-HT exist in raphe neurons that may contribute to the descending modulation of spinal sensory systems (e.g., GABA, glycine, acetylcholine, somatostatin, substance P, enkephalin, dynorphin, galanin, thyrotropin-releasing hormone, and cholecystokinin) (Millan, 2002). The present study focused on the inhibitory inputs to the SG neurons by using the *in vivo* spinal cord patch-clamp technique and revealed that the RVM-ES evoked monosynaptic GABAergic and glycinergic responses in >50% of the SG neurons that were tested. In current-clamp mode, the facilitation of the inhibitory inputs effectively blocked the action potentials of the SG neurons elicited by the mechanical noxious stimuli to the skin. Among the multiple neuromodulatory pathways in the raphe-spinal system that have been revealed by neuroanatomical studies (Millhorn et al., 1987, 1988; Jones et al., 1991; Sorkin et al., 1993; Antal et al., 1996; Millan, 2002), our report demonstrates functional evidence of the direct GABAergic and glycinergic pathways to the SG.

Under *in vivo* conditions, the basal frequency of IPSCs (~35 Hz) was much higher than that reported in the spinal dorsal horn neurons in transverse spinal cord slice preparations (<5 Hz) (Nakatsuka et al., 2005). This may be because of the presence of inputs from supraspinal structures, other spinal segments, and peripheral nerves. Electrical stimulation of the brain activates not only the neuronal somas, but also axonal fibers passing through the stimulation sites; however, the present results indicated that not only RVM-ES but also RVM-GI produced facilitation of IPSCs, suggesting that an activation of the RVM neurons induced the responses. As shown in Figure 2, RVM-GI produced a prolonged increase in sIPSC frequency and amplitude, whereas RVM-ES induced stimulus-locked responses (Fig. 3*A*). The reason for the difference may be that the infused glutamate diffuses from the tip of the cannula in the parenchyma and stimulates the RVM neurons even after cessation of the microinjection.

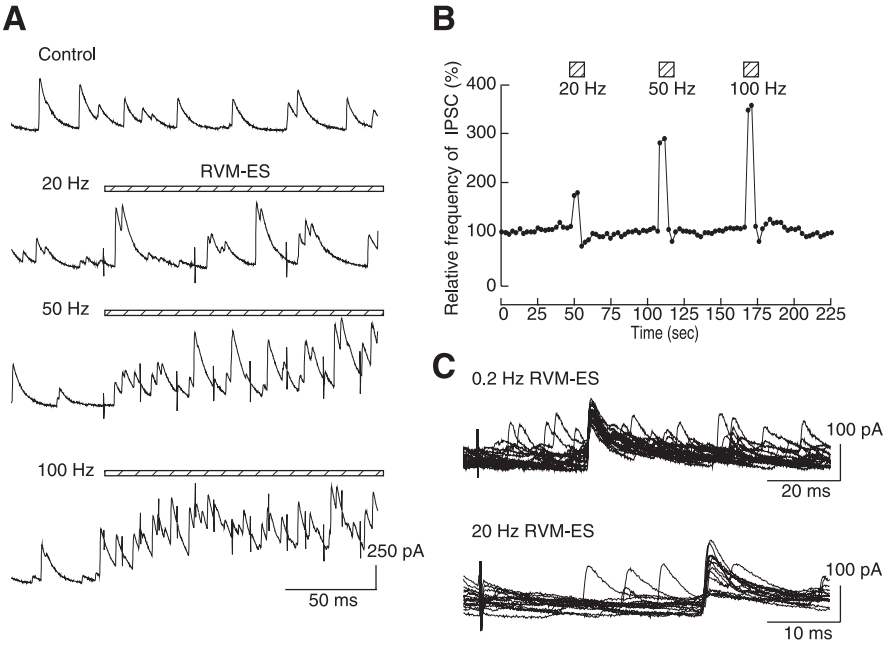

Figure 6. Monosynaptically evoked IPSCs by RVM-ES. ***A***, The frequency of IPSCs was increased in a stimulus-frequency-dependent manner. The RVM-ES was always accompanied by IPSCs. ***B***, Stimulus-frequency-dependent increase in relative frequency of IPSCs with the RVM-ES at 20, 50, and 100 Hz (100 μA). ***C***, Superimposed traces of IPSCs evoked at 0.2 Hz (top) and 20 Hz (bottom) RVM-ES, respectively. Note that IPSCs were evoked at fixed latency and showed no failures. Holding potential: 0 mV.

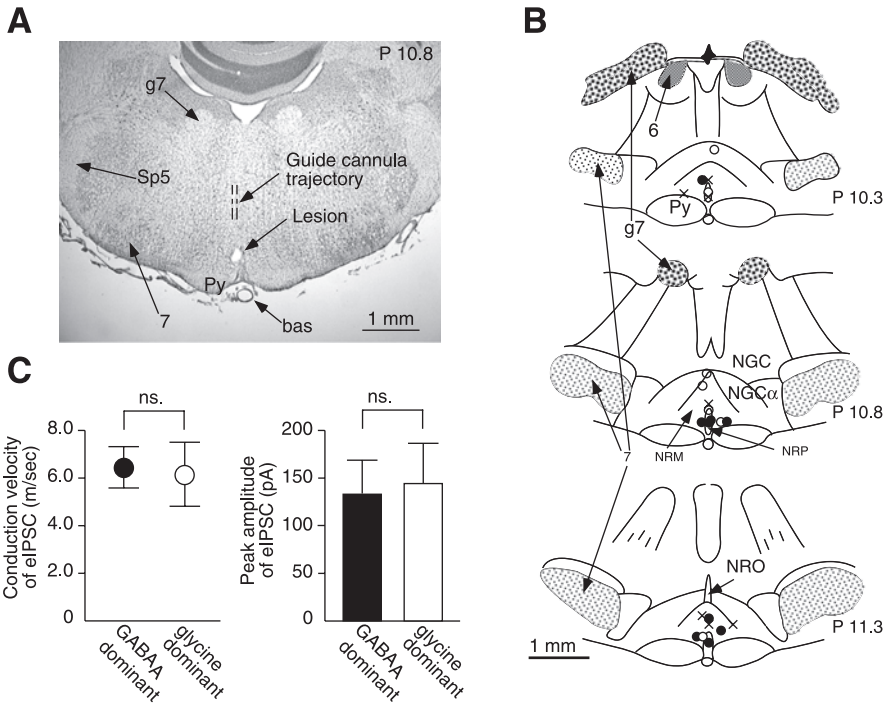

Figure 7. Stimulation sites of the RVM-ES. ***A***, Example of a photomicrograph of a 50-μm-thick coronal section with a small electrolytic lesion marking a stimulation site in the RVM. ***B***, Stimulation sites illustrated on representative coronal brain sections (Paxinos and Watson, 2005). Filled and open circles indicate the stimulation sites eliciting $GABA_A$- and glycine-dominant eIPSCs, respectively. X indicates the sites eliciting no significant responses. py, Pyramidal tract; 6, abducens nucleus; 7, facial nucleus; g7, genu of the facial nerve; NRO, nucleus raphe obscurus; Sp5, spinal trigeminal tract. The caudal distance of each section from bregma is indicated by values next to P (in millimeters). ***C***, CV (left) and peak amplitudes (right) of GABAergic ($n = 12$) and glycinergic ($n = 6$) IPSCs.

It has been reported that electrical stimulation of the NRM evokes an increase in postsynaptic conductance that leads to hyperpolarization of the neurons in spinal laminas I and II in *in vivo* intracellular recordings, suggesting an increase in chloride or potassium permeability (Light et al., 1986); however, because no slow outward or inward current was observed when we recorded

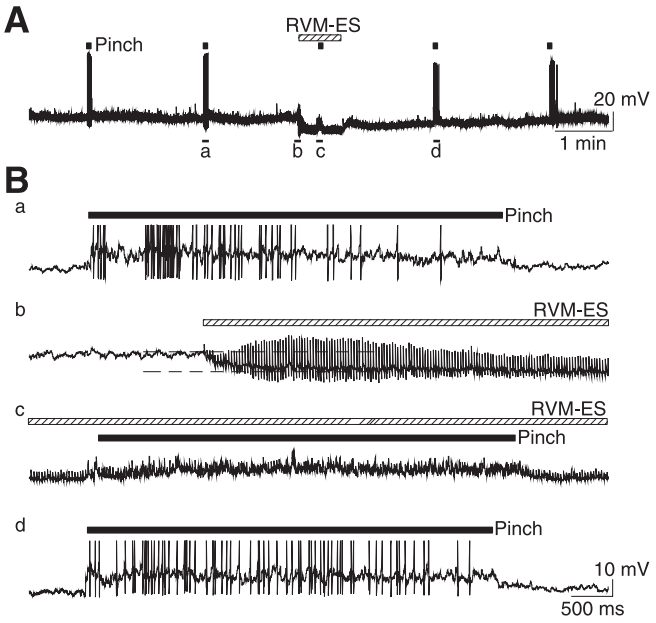

Figure 8. Suppression of the pinch-induced responses by the RVM-ES. ***A***, Five sets of pinch stimuli for 5 s (black squares) were applied every 2 min to the receptive field of the ipsilateral hindlimb, and the RVM-ES was applied from 30 s before the third pinch stimulus for 1 min in current-clamp mode. ***Ba–Bd*** correspond to ***Aa–Ad*** on an expanded time scale. ***Ba***, Pinch stimulation produced a depolarization accompanied by a barrage of action potentials under current-clamp condition. Resting membrane potential was −62 mV. ***Bb***, RVM-ES (hatched square; 100 μA; 30 Hz) hyperpolarized the membrane potential, although 30 Hz artifacts overlapped. ***Bc***, RVM-ES suppressed action potentials elicited by pinch stimulation. ***Bd***, Action potentials were evoked again by pinch in the absence of RVM-ES

with the K-gluconate-containing pipette solution in our study, it is unlikely that the RVM-ES induces changes in potassium permeability. Alternatively, the present study demonstrated that the activation of the RVM enhanced IPSCs, which were GABAergic and glycinergic but not serotonergic. It is possible that the RVM-GI- and RVM-ES-induced facilitation of GABAergic and glycinergic IPSCs is mediated by certain neurotransmitters through polysynaptic pathways that activate local GABAergic and glycinergic neurons in the SG. For example, acetylcholine elicits an increase in GABA–glycine-mediated inhibitory activity in the SG (Baba et al., 1998; Takeda et al., 2003). Furthermore, 5-HT_3, as well as other types of serotonergic receptors, have been suggested to increase GABA release in the spinal dorsal horn (Alhaider et al., 1991; Peng et al., 2001; Hains et al., 2003; Kawamata et al., 2003); however, the facilitation of IPSCs induced by the RVM-ES with an intensity that was within the range of the previous RVM-ES studies (Light et al., 1986; Zhuo and Gebhart, 1997) was not blocked by antagonists of 5-HT_3 and other serotonergic receptor antagonists. These findings suggest that polysynaptic pathways involving 5-HT_3 ionotropic and/or other G-protein-coupled 5-HT receptors are not included in the RVM-ES-induced facilitation of IPSCs.

Neuroanatomical studies that used the retrograde tracing method from the lumbar spinal cord have revealed that a large population (73%) of the neurons in the pararaphe nuclei, such as NGC and NGCα, are not serotonergic (Jones et al., 1991), and there are direct projections of GABA- and glycine-containing axons from the RVM to the spinal dorsal horn (Antal et al., 1996). Our results showed a fixed latency and no failure at high stimulus frequency of the RVM-ES-eIPSCs that was not abolished by AMPA and NMDA receptor antagonists or 5-HT antagonists (Figs. 4, 5). These findings suggest that the RVM-ES-eIPSCs were not polysynaptic but monosynaptic GABAergic and glycinergic, being compatible with the neuroanatomical studies. It has been reported that 5-HT-containing axons in the dorsolateral funiculus of the spinal cord that derive from NRM neurons are unmyelinated fibers (Basbaum et al., 1988). Our finding that the conduction velocity of the RVM-ES-eIPSCs was within the range of myelinated fibers may again support the suggestion that eIPSCs are not mediated by serotonergic fibers; however, the presence of polysynaptic pathways mediated by other neurotransmitters such as 5-HT was not excluded, because in a few cases (12%; 2 of 17) the facilitation of IPSCs continued after the cessation of the RVM-ES.

Reichling and Basbaum (1990) have reported that, although GABA-immunoreactive neurons are abundant in the RVM, those sending axons to the spinal dorsal horn are unevenly distributed in the RVM; i.e., only 2% of retrogradely labeled neurons are in the NRM, whereas 6–15 and 15–30% of retrogradely labeled neurons are in the pararaphe nuclei (NGC and NGCα, respectively). Furthermore, it has been suggested that chemical activation of bulbospinal GABAergic neurons in the NGCα is more likely to induce antinociceptive effects than those in the NRM (McGowan and Hammond, 1993). In the present study, because we aimed mainly at the raphe nuclei in the RVM, 21 of 23 ($>$90%) of the stimulating sites were located in the raphe nuclei (NRM and NRP) and only 2 were in the NGCα. Nevertheless, not only NGCα but also $>$75% (16 of 21) of the raphe stimulation elicited monosynaptic GABAergic or glycinergic IPSCs. It is considered that the largest current spread can be calculated to activate medullospinal neurons up to 1 mm away from the electrode at a stimulus intensity of 100 μA (Hentall and Fields, 1979). Therefore, it is possible that monosynaptic IPSCs in the present study were evoked by cell bodies or fibers in the pararaphe nuclei, although the tip of the electrode was located in the raphe nuclei.

The average amplitudes of both GABAergic and glycinergic IPSCs evoked by the RVM-ES (133 $\pm$ 34.9 and 144 $\pm$ 41.9 pA, respectively) are almost the same as those of dorsal horn-evoked monosynaptic IPSCs recorded from SG neurons in the slice preparations (Kohno et al., 2000), suggesting that the inhibitory inputs from the RVM have a significant role in the SG. In fact, the pinch-evoked action potentials in SG neurons were substantially suppressed by hyperpolarization produced by the RVM-ES (Fig. 8). In conclusion, it is suggested that the descending monosynaptic inhibitory inputs from the RVM demonstrated in the present study take part in antinociception against the noxious mechanical stimuli by suppressing SG neurons.

References

Alhaider AA, Lei SZ, Wilcox GL (1991) Spinal 5-HT_3 receptor-mediated antinociception: possible release of GABA. J Neurosci 11:1881–1888.

Antal M, Petko M, Polgar E, Heizmann CW, Storm-Mathisen J (1996) Direct evidence of an extensive GABAergic innervation of the spinal dorsal horn by fibres descending from the rostral ventromedial medulla. Neuroscience 73:509–518.

Azami J, Llewelyn MB, Roberts MH (1982) The contribution of nucleus reticularis paragigantocellularis and nucleus raphe magnus to the analgesia produced by systemically administered morphine, investigated with the microinjection technique. Pain 12:229–246.

Baba H, Kohno T, Okamoto M, Goldstein PA, Shimoji K, Yoshimura M (1998) Muscarinic facilitation of GABA release in substantia gelatinosa of the rat spinal dorsal horn. J Physiol (Lond) 508:83–93.

Basbaum AI, Zahs K, Lord B, Lakos S (1988) The fiber caliber of 5-HT immunoreactive axons in the dorsolateral funiculus of the spinal cord of the rat and cat. Somatosens Res 5:177–185.

Beal J, Bicknell HRJ (1985) Development and maturation of neurons in the

substantia gelatinosa (SG) of the rat spinal cord. In: Development, organization, and processing in somatosensory pathways (Rowe M, Willis WDJ, eds), pp 23–30. New York: Wiley.

Belcher G, Ryall RW, Schaffner R (1978) The differential effects of 5-hydroxytryptamine, noradrenaline and raphe stimulation on nociceptive and non-nociceptive dorsal horn interneurones in the cat. Brain Res 151:307–321.

Bowker RM, Abbott LC (1988) The origins and trajectories of somatostatin reticulospinal neurons: a potential neurotransmitter candidate of the dorsal reticulospinal pathway. Brain Res 447:398–403.

Bowker RM, Westlund KN, Coulter JD (1981) Origins of serotonergic projections to the spinal cord in rat: an immunocytochemical-retrograde transport study. Brain Res 226:187–199.

Brodie MS, Proudfit HK (1984) Hypoalgesia induced by the local injection of carbachol into the nucleus raphe magnus. Brain Res 291:337–342.

Carstens E, Bihl H, Irvine DR, Zimmermann M (1981) Descending inhibition from medial and lateral midbrain of spinal dorsal horn neuronal responses to noxious and nonnoxious cutaneous stimuli in the cat. J Neurophysiol 45:1029–1042.

Cervero F, Iggo A (1980) The substantia gelatinosa of the spinal cord: a critical review. Brain 103:717–772.

Duggan AW, Griersmith BT (1979) Inhibition of the spinal transmission of nociceptive information by supraspinal stimulation in the cat. Pain 6:149–161.

Fields HL, Basbaum AI, Clanton CH, Anderson SD (1977) Nucleus raphe magnus inhibition of spinal cord dorsal horn neurons. Brain Res 126:441–453.

Furue H, Narikawa K, Kumamoto E, Yoshimura M (1999) Responsiveness of rat substantia gelatinosa neurones to mechanical but not thermal stimuli revealed by in vivo patch-clamp recording. J Physiol (Lond) 521:529–535.

Hains BC, Willis WD, Hulsebosch CE (2003) Serotonin receptors 5-HT1A and 5-HT3 reduce hyperexcitability of dorsal horn neurons after chronic spinal cord hemisection injury in rat. Exp Brain Res 149:174–186.

Hentall ID, Fields HL (1979) Segmental and descending influences on intraspinal thresholds of single C-fibers. J Neurophysiol 42:1527–1537.

Hodge Jr CJ, Apkarian AV, Owen MP, Hanson BS (1983) Changes in the effects of stimulation of locus coeruleus and nucleus raphe magnus following dorsal rhizotomy. Brain Res 288:325–329.

Jones BE, Holmes CJ, Rodriguez-Veiga E, Mainville L (1991) GABA-synthesizing neurons in the medulla: their relationship to serotonin-containing and spinally projecting neurons in the rat. J Comp Neurol 313:349–367.

Kawamata T, Omote K, Toriyabe M, Yamamoto H, Namiki A (2003) The activation of 5-HT(3) receptors evokes GABA release in the spinal cord. Brain Res 978:250–255.

Kohno T, Kumamoto E, Baba H, Ataka T, Okamoto M, Shimoji K, Yoshimura M (2000) Actions of midazolam on GABAergic transmission in substantia gelatinosa neurons of adult rat spinal cord slices. Anesthesiology 92:507–515.

Kumazawa T, Perl ER (1978) Excitation of marginal and substantia gelatinosa neurons in the primate spinal cord: indications of their place in dorsal horn functional organization. J Comp Neurol 177:417–434.

Light AR, Casale EJ, Menetrey DM (1986) The effects of focal stimulation in nucleus raphe magnus and periaqueductal gray on intracellularly recorded neurons in spinal laminae I and II. J Neurophysiol 56:555–571.

McGowan MK, Hammond DL (1993) Antinociception produced by microinjection of L-glutamate into the ventromedial medulla of the rat: mediation by spinal GABAA receptors. Brain Res 620:86–96.

Millan MJ (2002) Descending control of pain. Prog Neurobiol 66:355–474.

Millhorn DE, Hokfelt T, Seroogy K, Oertel W, Verhofstad AA, Wu JY (1987) Immunohistochemical evidence for colocalization of gamma-aminobutyric acid and serotonin in neurons of the ventral medulla oblongata projecting to the spinal cord. Brain Res 410:179–185.

Millhorn DE, Hokfelt T, Seroogy K, Verhofstad AA (1988) Extent of colocalization of serotonin and GABA in neurons of the ventral medulla oblongata in rat. Brain Res 461:169–174.

Nakatsuka T, Chen M, Takeda D, King C, Ling J, Xing H, Ataka T, Vierck C, Yezierski R, Gu JG (2005) Substance P-driven feed-forward inhibitory activity in the mammalian spinal cord. Mol Pain 1:20.

Narikawa K, Furue H, Kumamoto E, Yoshimura M (2000) In vivo patch-clamp analysis of IPSCs evoked in rat substantia gelatinosa neurons by cutaneous mechanical stimulation. J Neurophysiol 84:2171–2174.

Oleson TD, Twombly DA, Liebeskind JC (1978) Effects of pain-attenuating brain stimulation and morphine on electrical activity in the raphe nuclei of the awake rat. Pain 4:211–230.

Paxinos G, Watson C (2005) The rat brain in stereotaxic coordinates, Ed 5. San Diego: Academic.

Peng YB, Wu J, Willis WD, Kenshalo DR (2001) GABA(A) and 5-HT(3) receptors are involved in dorsal root reflexes: possible role in periaqueductal gray descending inhibition. J Neurophysiol 86:49–58.

Reddy VK, Cassini P, Ho RH, Martin GF (1990) Origins and terminations of bulbospinal axons that contain serotonin and either enkephalin or substance-P in the North American opossum. J Comp Neurol 294:96–108.

Reichling DB, Basbaum AI (1990) Contribution of brainstem GABAergic circuitry to descending antinociceptive controls: I. GABA-immunoreactive projection neurons in the periaqueductal gray and nucleus raphe magnus. J Comp Neurol 302:370–377.

Rexed B (1952) The cytoarchitectonic organization of the spinal cord in the cat. J Comp Neurol 96:414–495.

Rivot JP, Chaouch A, Besson JM (1980) Nucleus raphe magnus modulation of response of rat dorsal horn neurons to unmyelinated fiber inputs: partial involvement of serotonergic pathways. J Neurophysiol 44:1039–1057.

Silverman JD, Kruger L (1990) Selective neuronal glycoconjugate expression in sensory and autonomic ganglia: relation of lectin reactivity to peptide and enzyme markers. J Neurocytol 19:789–801.

Sonohata M, Furue H, Katafuchi T, Yasaka T, Doi A, Kumamoto E, Yoshimura M (2004) Actions of noradrenaline on substantia gelatinosa neurones in the rat spinal cord revealed by in vivo patch recording. J Physiol (Lond) 555:515–526.

Sorkin LS, McAdoo DJ, Willis WD (1993) Raphe magnus stimulation-induced antinociception in the cat is associated with release of amino acids as well as serotonin in the lumbar dorsal horn. Brain Res 618:95–108.

Sugiura Y, Lee CL, Perl ER (1986) Central projections of identified, unmyelinated (C) afferent fibers innervating mammalian skin. Science 234:358–361.

Takeda D, Nakatsuka T, Papke R, Gu JG (2003) Modulation of inhibitory synaptic activity by a non-a4b2, non-a7 subtype of nicotinic receptors in the substantia gelatinosa of adult rat spinal cord. Pain 101:13–23.

Woolf CJ, Fitzgerald M (1983) The properties of neurones recorded in the superficial dorsal horn of the rat spinal cord. J Comp Neurol 221:313–328.

Yoshimura M (1996) Slow synaptic transmission in the spinal dorsal horn. Prog Brain Res 113:443–462.

Yoshimura M, Jessell TM (1989) Primary afferent-evoked synaptic responses and slow potential generation in rat substantia gelatinosa neurons in vitro. J Neurophysiol 62:96–108.

Yoshimura M, Nishi S (1993) Blind patch-clamp recordings from substantia gelatinosa neurons in adult rat spinal cord slices: pharmacological properties of synaptic currents. Neuroscience 53:519–526.

Zhuo M, Gebhart GF (1997) Biphasic modulation of spinal nociceptive transmission from the medullary raphe nuclei in the rat. J Neurophysiol 78:746–758.